

¹ Critical transitions and the fragmenting of global forests

² Leonardo A. Saravia^{1 3}, Santiago R. Doyle¹, Benjamin Bond-Lamberty²

³ 1. Instituto de Ciencias, Universidad Nacional de General Sarmiento, J.M. Gutierrez 1159 (1613), Los
⁴ Polvorines, Buenos Aires, Argentina.

⁵ 2. Pacific Northwest National Laboratory, Joint Global Change Research Institute at the University of
⁶ Maryland–College Park, 5825 University Research Court #3500, College Park, MD 20740, USA

⁷ 3. Corresponding author e-mail: lsaravia@ungs.edu.ar

⁸ **Keywords:** Forest fragmentation, early warning signals, percolation, power-laws, MODIS, critical transitions

⁹ **Running title:** Critical fragmentation in global forest

¹⁰ Abstract

¹¹ 1. Forests provide critical habitat for many species, essential ecosystem services, and are coupled to
¹² atmospheric dynamics through exchanges of energy, water and gases. One of the most important
¹³ changes produced in the biosphere is the replacement of forest areas with human dominated landscapes.
¹⁴ This usually leads to fragmentation, altering the sizes of patches, the structure and function of the
¹⁵ forest. Here we studied the distribution and dynamics of forest patch sizes at a global level, examining
¹⁶ signals of a critical transition from an unfragmented to a fragmented state.

¹⁷ 2. We used MODIS vegetation continuous field to estimate the forest patches at a global level and defined
¹⁸ wide regions of connected forest across continents and big islands. We search for critical phase transi-
¹⁹ tions, where the system state of the forest changes suddenly at a critical point; this implies an abrupt
²⁰ change in connectivity that causes a increased fragmentation level. We studied the distribution of for-
²¹ est patch sizes and the dynamics of the largest patch over the last fourteen years. The conditions that
²² indicate that a region is near a critical fragmentation threshold are related to patch size distribution
²³ and temporal fluctuations of the largest patch.

²⁴ 3. We found that most regions, except the Eurasian mainland, followed a power-law distribution. Only
²⁵ the tropical forest of Africa and South America met the criteria to be near a critical fragmentation
²⁶ threshold.

²⁷ 4. This implies that human pressures and climate forcings might trigger undesired effects of fragmentation,
²⁸ such as species loss and degradation of ecosystems services, in these regions. The simple criteria

²⁹ proposed here could be used as early warning to estimate the distance to a fragmentation threshold in
³⁰ forest around the globe and could be used as a predictor of a planetary tipping point.

31 Introduction

32 Forests are one of the most important ecosystems on earth, providing habitat for a large proportion of species
33 and contributing extensively to global biodiversity (Crowther *et al.* 2015). In the previous century human
34 activities have influenced global bio-geochemical cycles (Bonan 2008; Canfield, Glazer & Falkowski 2010),
35 with one of the most dramatic changes being the replacement of 40% of Earth's formerly biodiverse land
36 areas with landscapes that contain only a few species of crop plants, domestic animals and humans (Foley
37 *et al.* 2011). These local changes have accumulated over time and now constitute a global forcing (Barnosky
38 *et al.* 2012).

39 Another global scale forcing that is tied to habitat destruction is fragmentation, which is defined as the
40 division of a continuous habitat into separated portions that are smaller and more isolated. Fragmentation
41 produces multiple interwoven effects: reductions of biodiversity between 13% and 75%, decreasing forest
42 biomass, and changes in nutrient cycling (Haddad *et al.* 2015). The effects of fragmentation are not only
43 important from an ecological point of view but also that of human activities, as ecosystem services are deeply
44 influenced by the level of landscape fragmentation (Mitchell *et al.* 2015).

45 Ecosystems have complex interactions between species and present feedbacks at different levels of organiza-
46 tion (Gilman *et al.* 2010), and external forcings can produce abrupt changes from one state to another,
47 called critical transitions (Scheffer *et al.* 2009). These abrupt state shifts cannot be linearly forecasted from
48 past changes, and are thus difficult to predict and manage (Scheffer *et al.* 2009). Critical transitions have
49 been detected mostly at local scales (Drake & Griffen 2010; Carpenter *et al.* 2011), but the accumulation of
50 changes in local communities that overlap geographically can propagate and theoretically cause an abrupt
51 change of the entire system at larger scales (Barnosky *et al.* 2012). Coupled with the existence of global
52 scale forcings, this implies the possibility that a critical transition could occur at a global scale (Rockstrom
53 *et al.* 2009; Folke *et al.* 2011).

54 Complex systems can experience two general classes of critical transitions (Solé 2011). In so-called first
55 order transitions, a catastrophic regime shift that is mostly irreversible occurs because of the existence of
56 alternative stable states (Scheffer *et al.* 2001). This class of transitions is suspected to be present in a variety
57 of ecosystems such as lakes, woodlands, coral reefs (Scheffer *et al.* 2001), semi-arid grasslands (Bestelmeyer
58 *et al.* 2011), and fish populations (Vasilakopoulos & Marshall 2015). They can be the result of positive
59 feedback mechanisms (Martín *et al.* 2015); for example, fires in some forest ecosystems were more likely to
60 occur in previously burned areas than in unburned places (Kitzberger *et al.* 2012).

61 The other class of critical transitions are continuous or second order transitions (Solé & Bascompte 2006).

62 In these cases, there is a narrow region where the system suddenly changes from one domain to another,
63 with the change being continuous and in theory reversible. This kind of transitions were suggested to be
64 present in tropical forest (Pueyo *et al.* 2010), semi-arid mountain ecosystems (McKenzie & Kennedy 2012),
65 tundra shrublands (Naito & Cairns 2015). The transition happens at critical point where we can observe a
66 distinctive spatial pattern: scale invariant fractal structures characterized by power law patch distributions
67 (Stauffer & Aharony 1994).

68 There are several processes that can convert a catastrophic transition to a second order transitions (Martín
69 *et al.* 2015). These include stochasticity, such as demographic fluctuations, spatial heterogeneities, and/or
70 dispersal limitation. All these components are present in forest around the globe (Seidler & Plotkin 2006;
71 Filotas *et al.* 2014; Fung *et al.* 2016), thus continuous transitions might be more probable than catastrophic
72 transitions. Moreover there is some evidence of recovery in some systems that supposedly suffered an
73 irreversible transition produced by overgrazing (Zhang *et al.* 2005) and desertification (Allington & Valone
74 2010).

75 The spatial phenomena observed in continuous critical transitions deal with connectivity, a fundamental
76 property of general systems and ecosystems from forests (Ochoa-Quintero *et al.* 2015) to marine ecosystems
77 (Leibold & Norberg 2004) and the whole biosphere (Lenton & Williams 2013). When a system goes from a
78 fragmented to a connected state we say that it percolates (Solé 2011). Percolation implies that there is a
79 path of connections that involves the whole system. Thus we can characterize two domains or phases: one
80 dominated by short-range interactions where information cannot spread, and another in which long range
81 interactions are possible and information can spread over the whole area. (The term “information” is used
82 in a broad sense and can represent species dispersal or movement.)

83 Thus, there is a critical “percolation threshold” between the two phases, and the system could be driven
84 close to or beyond this point by an external force; climate change and deforestation are the main forces
85 that could be the drivers of such a phase change in contemporary forests (Bonan 2008; Haddad *et al.* 2015).
86 There are several applications of this concept in ecology: species’ dispersal strategies are influenced by
87 percolation thresholds in three-dimensional forest structure (Solé, Bartumeus & Gamarra 2005), and it has
88 been shown that species distributions also have percolation thresholds (He & Hubbell 2003). This implies
89 that pushing the system below the percolation threshold could produce a biodiversity collapse (Bascompte
90 & Solé 1996; Solé, Alonso & Saldaña 2004; Pardini *et al.* 2010); conversely, being in a connected state (above
91 the threshold) could accelerate the invasion of forest into prairie (Loehle, Li & Sundell 1996; Naito & Cairns
92 2015).

93 One of the main challenges with systems that can experience critical transitions—of any kind—is that the

94 value of the critical threshold is not known in advance. In addition, because near the critical point a small
95 change can precipitate a state shift of the system, they are difficult to predict. Several methods have been
96 developed to detect if a system is close to the critical point, e.g. a deceleration in recovery from perturbations,
97 or an increase in variance in the spatial or temporal pattern (Hastings & Wysham 2010; Carpenter *et al.*
98 2011; Boettiger & Hastings 2012; Dai *et al.* 2012).

99 In this study, our objective is to look for evidence that forests around the globe are near continuous critical
100 point that represent a fragmentation threshold. We use the framework of percolation to first evaluate if
101 forest patch distribution at a continental scale is described by a power law distribution and then examined
102 the fluctuations of the largest patch. The advantage of using data at a continental scale is that for very large
103 systems the transitions are very sharp (Solé 2011) and thus much easier to detect than at smaller scales,
104 where noise can mask the signals of the transition.

105 Methods

106 Study areas definition

107 We analyzed mainland forests at a continental scale, covering the whole globe, by delimiting land areas with
108 a near-contiguous forest cover, separated with each other by large non-forested areas. Using this criterion,
109 we delimited the following forest regions. In America, three regions were defined: South America temperate
110 forest (SAT), subtropical and tropical forest up to Mexico (SAST), and USA and Canada forest (NA). Europe
111 and North Asia were treated as one region (EUAS). The rest of the delimited regions were South-east Asia
112 (SEAS), Africa (AF), and Australia (OC). We also included in the analysis islands larger than 10^5 km². The
113 mainland region has the number 1 e.g. OC1, and the nearby islands have consecutive numeration (Appendix
114 S4, figure S1-S6).

115 Forest patch distribution

116 We studied forest patch distribution in each defined area from 2000 to 2014 using the MODerate-resolution
117 Imaging Spectroradiometer (MODIS) Vegetation Continuous Fields (VCF) Tree Cover dataset version 051
118 (DiMiceli *et al.* 2015). This dataset is produced at a global level with a 231-m resolution, from 2000 onwards
119 on an annual basis. There are several definition of forest based on percent tree cover (Sexton *et al.* 2015),
120 we choose a 30% threshold to convert the percentage tree cover to a binary image of forest and non-forest
121 pixels. This was the definition used by the United Nations' International Geosphere-Biosphere Programme
122 (Belward 1996), and studies of global fragmentation (Haddad *et al.* 2015). This definition avoids the errors

123 produced by low discrimination of MODIS VCF between forest and dense herbaceous vegetation at low forest
124 cover (Sexton *et al.* 2015). Patches of contiguous forest were determined in the binary image by grouping
125 connected forest pixels using a neighborhood of 8 forest units (Moore neighborhood).

126 **Percolation theory**

127 A more in-depth introduction to percolation theory can be found elsewhere (Stauffer & Aharony 1994) and
128 a review from an ecological point of view is available (Oborny, Szabó & Meszéna 2007). Here, to explain
129 the basic elements of percolation theory we formulate a simple model: we represent our area of interest by a
130 square lattice and each site of the lattice can be occupied—e.g. by forest—with a probability p . The lattice
131 will be more occupied when p is greater, but the sites are randomly distributed. We are interested in the
132 connection between sites, so we define a neighborhood as the eight adjacent sites surrounding any particular
133 site. The sites that are neighbors of other occupied sites define a patch. When there is a patch that connects
134 the lattice from opposite sides, it is said that the system percolates. When p is increased from low values, a
135 percolating patch suddenly appears at some value of p called the critical point p_c .

136 Thus percolation is characterized by two well defined phases: the unconnected phase when $p < p_c$ (called
137 subcritical in physics), in which species cannot travel far inside the forest, as it is fragmented; in a general
138 sense, information cannot spread. The second is the connected phase when $p > p_c$ (supercritical), species
139 can move inside a forest patch from side to side of the area (lattice), i.e. information can spread over the
140 whole area. Near the critical point several scaling laws arise: the structure of the patch that spans the area
141 is fractal, the size distribution of the patches is power-law, and other quantities also follow power-law scaling
142 (Stauffer & Aharony 1994).

143 The value of the critical point p_c depends on the geometry of the lattice and on the definition of the
144 neighborhood, but other power-law exponents only depend on the lattice dimension. Close to the critical
145 point, the distribution of patch sizes is:

146 (1) $n_s(p_c) \propto s^{-\alpha}$

147 where $n_s(p)$ is the number of patches of size s . The exponent α does not depend on the details of the
148 model and it is called universal (Stauffer & Aharony 1994). These scaling laws can be applied for landscape
149 structures that are approximately random, or at least only correlated over short distances (Gastner *et al.*
150 2009). In physics this is called “isotropic percolation universality class”, and corresponds to an exponent
151 $\alpha = 2.05495$. If we observe that the patch size distribution has another exponent it will not belong to this
152 universality class and some other mechanism should be invoked to explain it. Percolation thresholds can also

153 be generated by models that have some kind of memory (Hinrichsen 2000; Ódor 2004): for example, a patch
154 that has been exploited for many years will recover differently than a recently deforested forest patch. In
155 this case, the system could belong to a different universality class, or in some cases there is no universality,
156 in which case the value of α will depend on the parameters and details of the model (Corrado, Cherubini &
157 Pennetta 2014).

158 To illustrate these concepts, we conducted simulations with a simple forest model with only two states:
159 forest and non-forest. This type of model is called a “contact process” and was introduced for epidemics
160 (Harris 1974), but has many applications in ecology (Solé & Bascompte 2006; Gastner *et al.* 2009). A site
161 with forest can become extinct with probability e , and produce another forest site in a neighborhood with
162 probability c . We use a neighborhood defined by an isotropic power law probability distribution. We defined
163 a single control parameter as $\lambda = c/e$ and ran simulations for the subcritical fragmentation state $\lambda < \lambda_c$,
164 with $\lambda = 2$, near the critical point for $\lambda = 2.5$, and for the supercritical state with $\lambda = 5$ (see Appendix S2,
165 gif animations).

166 Patch size distributions

167 We fitted the empirical distribution of forest patch areas, based on the MODIS-derived data described above,
168 to four distributions using maximum likelihood estimation (Goldstein, Morris & Yen 2004; Clauset, Shalizi
169 & Newman 2009). The distributions were: power-law, power-law with exponential cut-off, log-normal, and
170 exponential. We assumed that the patch size distribution is a continuous variable that was discretized by
171 remote sensing data acquisition procedure.

172 We set a minimal patch size (X_{min}) at nine pixels to fit the patch size distributions to avoid artifacts at patch
173 edges due to discretization (Weerman *et al.* 2012). Besides this hard X_{min} limit we set due to discretization,
174 the power-law distribution needs a lower bound for its scaling behavior. This lower bound is also estimated
175 from the data by maximizing the Kolmogorov-Smirnov (KS) statistic, computed by comparing the empirical
176 and fitted cumulative distribution functions (Clauset *et al.* 2009). We also calculated the uncertainty of the
177 parameters using a non-parametric bootstrap method (Efron & Tibshirani 1994), and computed corrected
178 Akaike Information Criteria (AIC_c) and Akaike weights for each model (Burnham & Anderson 2002). Akaike
179 weights (w_i) are the weight of evidence in favor of model i being the actual best model given that one of the
180 N models must be the best model for that set of N models.

181 Additionally, we computed the goodness of fit of the power-law model following the bootstrap approach
182 described by Clauset et. al (2009), where simulated data sets following the fitted model are generated, and a

183 p -value computed as the proportion of simulated data sets that has a KS statistic less extreme than empirical
184 data. The criterion to reject the power law model suggested by Clauset et. al (2009) was $p \leq 0.1$, but as we
185 have a very large n , meaning that negligible small deviations could produce a rejection (Klaus, Yu & Plenz
186 2011), we chose a $p \leq 0.05$ to reject the power law model.

187 To test for differences between the fitted power law exponent for each study area we used a generalized least
188 squares linear model (Zuur *et al.* 2009) with weights and a residual auto-correlation structure. Weights were
189 the bootstrapped 95% confidence intervals and we added an auto-regressive model of order 1 to the residuals
190 to account for temporal autocorrelation.

191 **Largest patch dynamics**

192 The largest patch is the one that connects the highest number of sites in the area. This has been used
193 extensively to indicate fragmentation (Gardner & Urban 2007; Ochoa-Quintero *et al.* 2015). The relation of
194 the size of the largest patch S_{max} to critical transitions has been extensively studied in relation to percolation
195 phenomena (Stauffer & Aharony 1994; Bazant 2000; Botet & Ploszajczak 2004), but seldom used in ecological
196 studies (for an exception see Gastner *et al.* (2009)). When the system is in a connected state ($p > p_c$) the
197 landscape is almost insensitive to the loss of a small fraction of forest, but close to the critical point a minor
198 loss can have important effects (Solé & Bascompte 2006; Oborny *et al.* 2007), because at this point the
199 largest patch will have a filamentary structure, i.e. extended forest areas will be connected by thin threads.
200 Small losses can thus produce large fluctuations.

201 One way to evaluate the fragmentation of the forest is to calculate the proportion of the largest patch against
202 the total area (Keitt, Urban & Milne 1997). The total area of the regions we are considering (Appendix S4,
203 figures S1-S6) may not be the same than the total area that the forest could potentially occupy, thus a more
204 accurate way to evaluate the weight of S_{max} is to use the total forest area, that can be easily calculated
205 summing all the forest pixels. We calculate the proportion of the largest patch for each year, dividing S_{max}
206 by the total forest area of the same year: $RS_{max} = S_{max} / \sum_i S_i$. This has the effect of reducing the S_{max}
207 fluctuations produced due to environmental or climatic changes influences in total forest area. When the
208 proportion RS_{max} is large (more than 60%) the largest patch contains most of the forest so there are fewer
209 small forest patches and the system is probably in a connected phase. Conversely, when it is low (less than
210 20%), the system is probably in a fragmented phase (Saravia & Momo 2017).

211 The RS_{max} is a useful qualitative index that does not tell us if the system is near or far from the critical
212 transition; this can be evaluated using the temporal fluctuations. We calculate the fluctuations around the

mean with the absolute values $\Delta S_{max} = S_{max}(t) - \langle S_{max} \rangle$, using the proportions of RS_{max} . To characterize fluctuations we fitted three empirical distributions: power-law, log-normal, and exponential, using the same methods described previously. We expect that large fluctuation near a critical point have heavy tails (log-normal or power-law) and that fluctuations far from a critical point have exponential tails, corresponding to Gaussian processes (Rooij *et al.* 2013). As the data set spans 15 years, we do not have enough power to reliably detect which distribution is better (Clauset *et al.* 2009). To improve this we performed the goodness of fit test described above for all the distributions. We generated animated maps showing the fluctuations of the two largest patches to aid in the interpretations of the results.

A robust way to detect if the system is near a critical transition is to analyze the increase in variance of the density (Benedetti-Cecchi *et al.* 2015). It has been demonstrated that the variance increase in density appears when the system is very close to the transition (Corrado *et al.* 2014), thus practically it does not constitute an early warning indicator. An alternative is to analyze the variance of the fluctuations of the largest patch ΔS_{max} : the maximum is attained at the critical point but a significant increase occurs well before the system reaches the critical point (Corrado *et al.* 2014). In addition, before the critical fragmentation, the skewness of the distribution of ΔS_{max} should be negative, implying that fluctuations below the average are more frequent. We characterized the increase in the variance using quantile regression: if variance is increasing the slopes of upper or/and lower quartiles should be positive or negative.

All statistical analyses were performed using the GNU R version 3.3.0 (R Core Team 2015), using code provided by Cosma R. Shalizi for fitting the power law with exponential cutoff model and the poweRlaw package (Gillespie 2015) for fitting the other distributions. For the generalized least squares linear model we used the R function gls from package nlme (Pinheiro *et al.* 2016); and we fitted quantile regressions using the R package quantreg (Koenker 2016). Image processing was done in MATLAB r2015b (The Mathworks Inc.). The complete source code for image processing and statistical analysis, and the patch size data files are available at figshare <http://dx.doi.org/10.6084/m9.figshare.4263905>.

Results

The figure 1 shows an example of the distribution of the biggest 200 patches for years 2000 and 2014, this distribution is highly variable, but the biggest patch usually maintains its place. Sometimes the biggest patch breaks and then big fluctuations in its size are observed, as we will analyze below. Smaller patches can merge or break more easily so they enter or leave the list of 200, and this is why there is a color change across years.

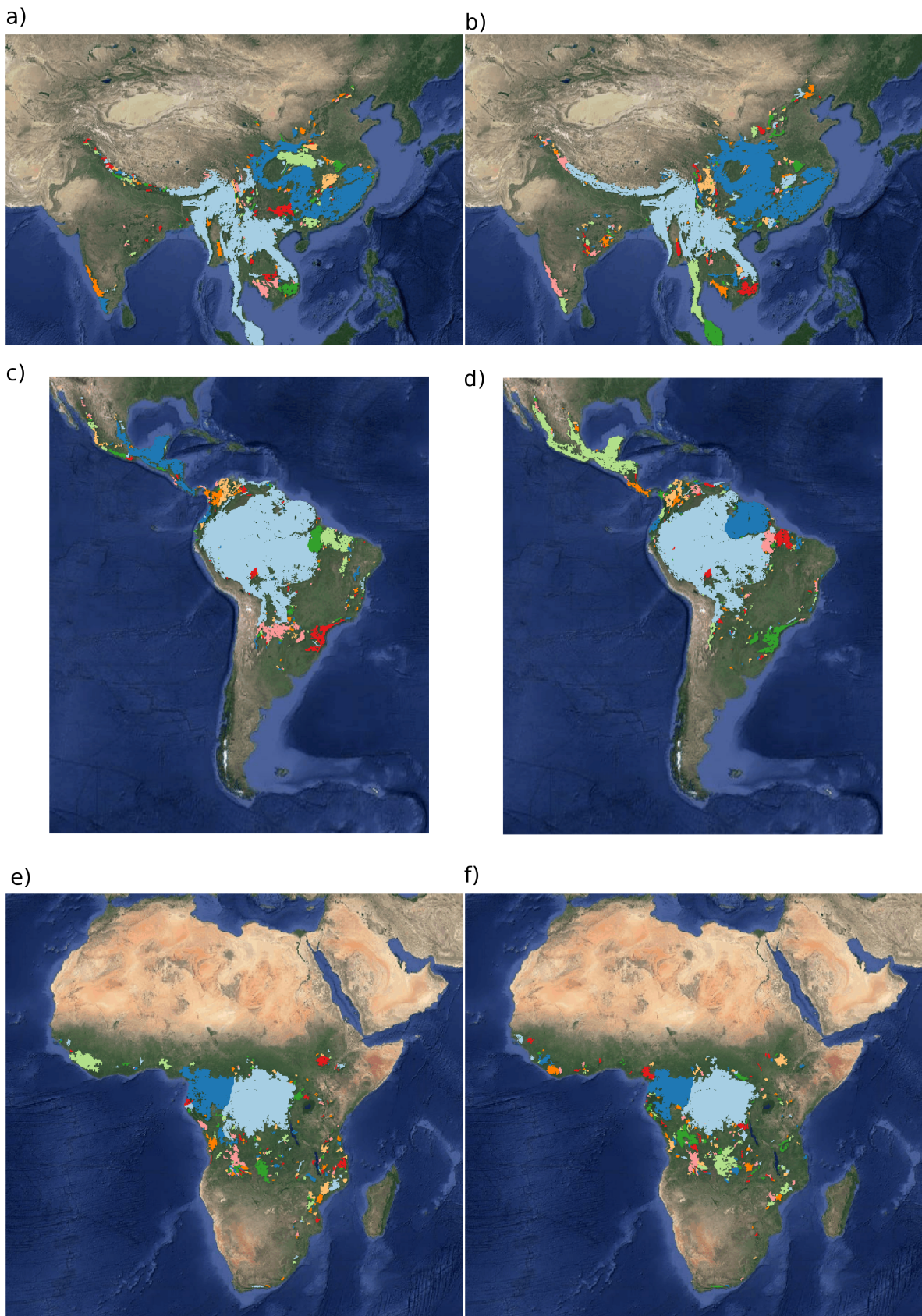


Figure 1: Forest patch distributions for continental regions for the years 2000 and 2014. The images are the 200 biggest patches, showed at a coarse pixel scale of 2.5 Km. The regions are: a) & b) southeast Asia; c) & d) South America subtropical and tropical and e) & f) Africa mainland, for the years 2000 and 2014 respectively.

243 The power law distribution was selected as the best model in 92% of the cases (Appendix S4, Figure S7).
244 In a small number of cases (1%) the power law with exponential cutoff was selected, but the value of the
245 parameter α was similar by ± 0.02 to the pure power law. Additionally the patch size where the exponential
246 tail begins is very large, thus we used the power law parameters for this cases (See Appendix S4, Figure S2,
247 region EUAS3). In finite-size systems the favored model should be the power law with exponential cutoff,
248 because the power-law tails are truncated to the size of the system (Stauffer & Aharony 1994). Here the
249 regions are so large that the cutoff is practically not observed.

250 There is only one region that did not follow a power law: Eurasia mainland, which showed a log-normal
251 distribution, representing 7% of the cases. The log-normal and power law are both heavy tailed distributions
252 and difficult to distinguish, but in this case Akaike weights have very high values for log-normal (near 1),
253 meaning that this is the only possible model. In addition, the goodness of fit tests clearly rejected the power
254 law model in all cases for this region (Appendix S4, table S1, region EUAS1). In general the goodness of fit
255 test rejected the power law model in fewer than 10% of cases. In large forest areas like Africa mainland (AF1)
256 or South America tropical-subtropical (SAST1), larger deviations are expected and the rejections rates are
257 higher so the proportion is 30% or less (Appendix S4, Table S1).

258 Taking into account the bootstrapped confidence intervals of each power law exponent (α) and the temporal
259 autocorrelation, there were no significant differences between α for the regions with the biggest (greater than
260 10^7 km^2) forest areas (Figure 2 and Appendix S4, Figure S8). There were also no differences between these
261 regions and smaller ones (Appendix S4, Tables S2 & S3), and all the slopes of α were not different from
262 0 (Appendix S4, Table S3). This implies a global average $\alpha = 1.908$, with a bootstrapped 95% confidence
263 interval between 1.898 and 1.920.

264 The proportion of the largest patch relative to total forest area RS_{max} for regions with more than 10^7 km^2
265 of forest is shown in figure 3. South America tropical and subtropical (SAST1) and North America (NA1)
266 have a higher RS_{max} of more than 60%, and other big regions 40% or less. For regions with less total
267 forest area (Appendix S4, figure S9 & Table 1), the United Kingdom (EUAS3) has a very low proportion
268 near 1%, while other regions such as New Guinea (OC2) and Malaysia/Kalimantan (OC3) have a very high
269 proportion. SEAS2 (Philippines) is a very interesting case because it seems to be under 30% until the year
270 2005, fluctuates in the range 30-60%, and then stays over 60% (Appendix S4, figure S9).

271 We analyzed the distributions of fluctuations of the largest patch relative to total forest area ΔRS_{max}
272 and the fluctuations of the largest patch ΔS_{max} . The model selection for ΔS_{max} resulted in power law
273 distributions for all regions (Appendix S4, table S6). For ΔRS_{max} instead some regions showed exponential
274 distributions: Eurasia mainland (EUAS1), New Guinea (OC2), Malaysia (OC3), New Zealand (OC6, OC8)

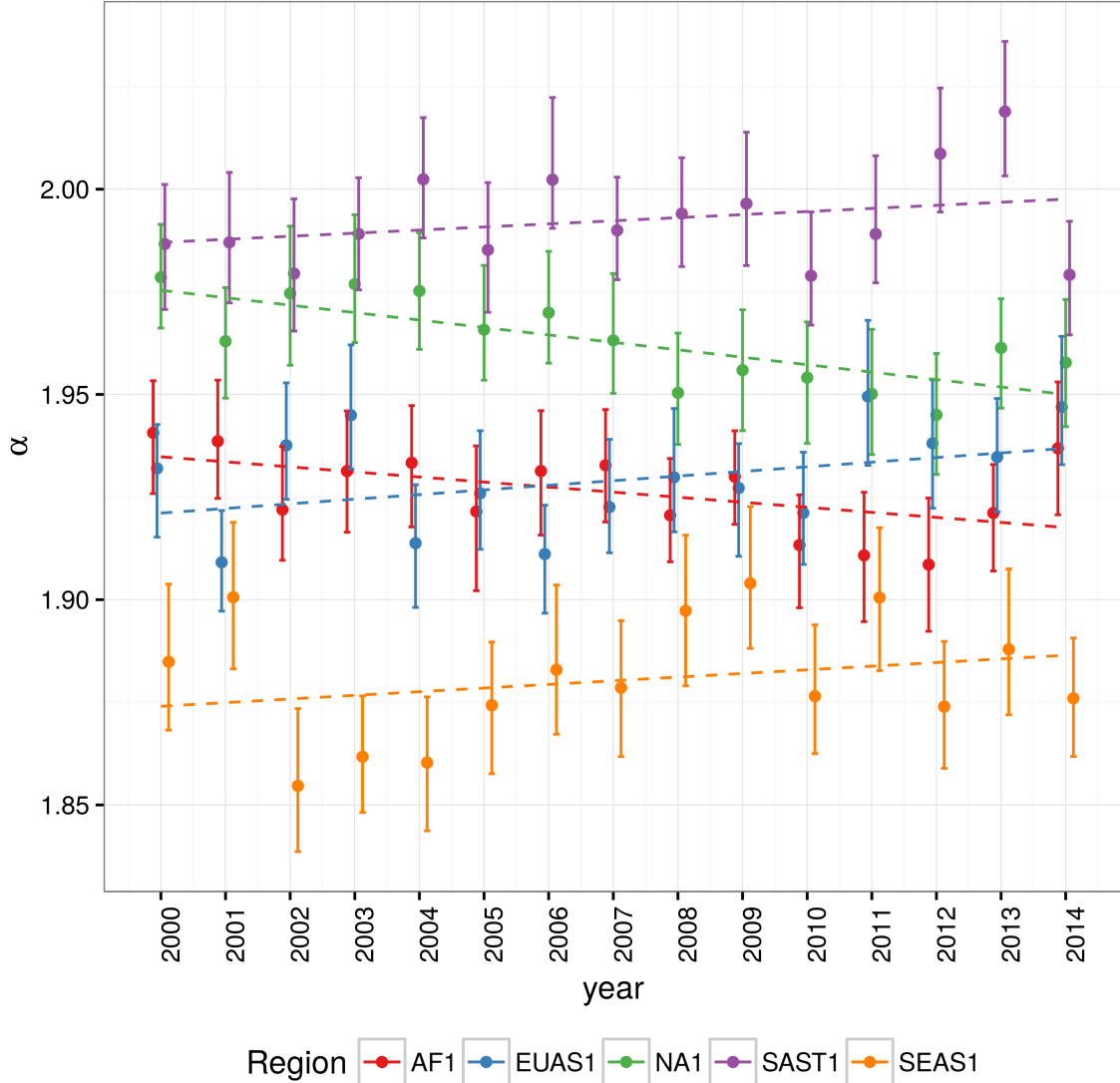


Figure 2: Power law exponents (α) of forest patch distributions for regions with total forest area $> 10^7 \text{ km}^2$. Dashed horizontal lines are the fitted generalized least squares linear model, with 95% confidence interval error bars estimated by bootstrap resampling. The regions are AF1: Africa mainland, EUAS1: Eurasia mainland, NA1: North America mainland, SAST1: South America subtropical and tropical, SEAS1: Southeast Asia mainland. For EUAS1 the best model is log-normal but the exponents are included here for comparison.

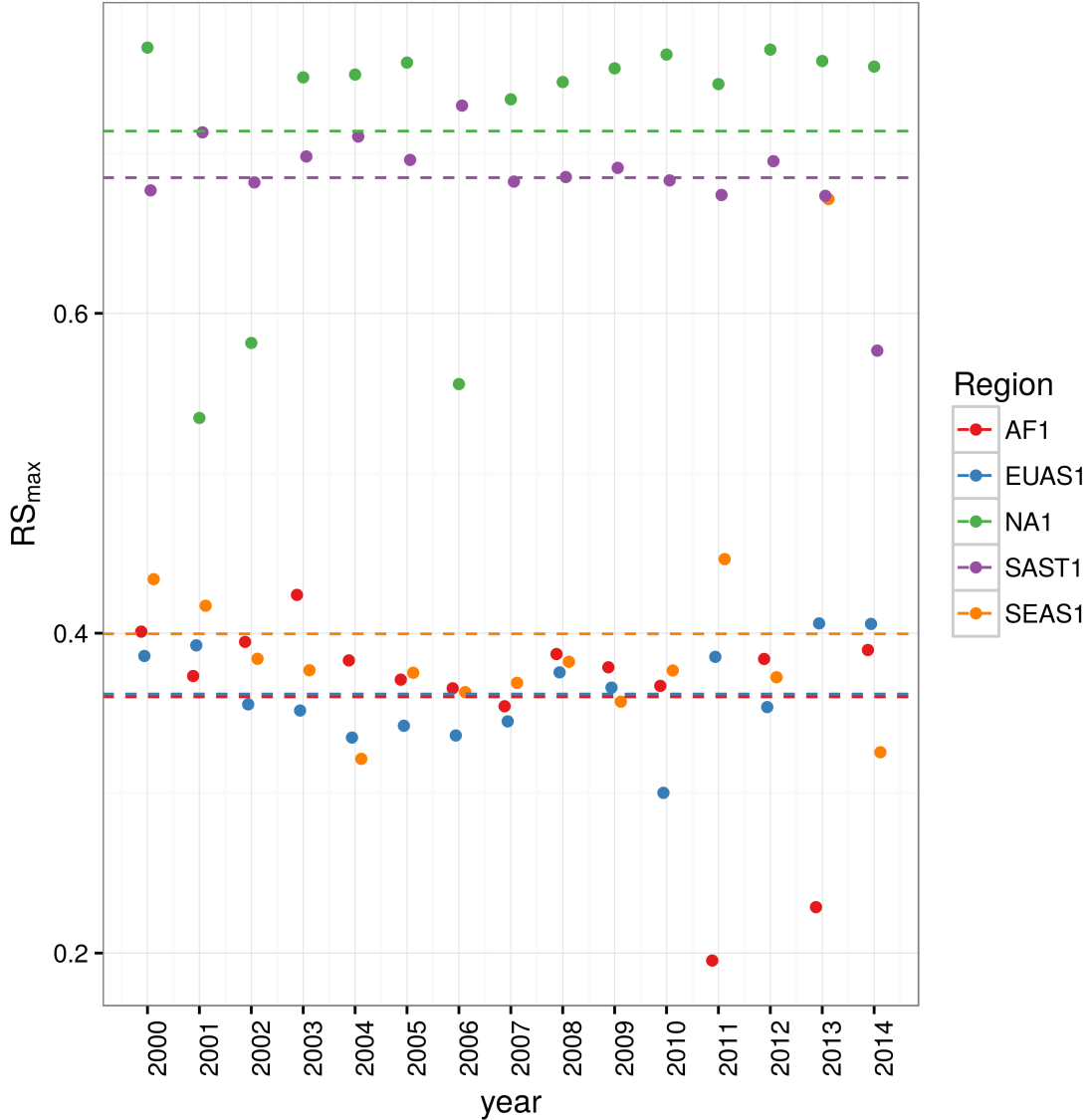


Figure 3: Largest patch proportion relative to total forest area RS_{max} , for regions with total forest area $> 10^7 \text{ km}^2$. Dashed lines are averages across time. The regions are AF1: Africa mainland, EUAS1: Eurasia mainland, NA1: North America mainland, SAST1: South America tropical and subtropical, SEAS1: Southeast Asia mainland.

275 and Java (OC7), all others were power laws (Appendix S4, Table S7). The goodness of fit test (GOF) did
276 not reject power laws in any case, but neither did it reject the other models except in a few cases; this was
277 due to the small number of observations. We only considered fluctuations to follow a power law when this
278 distribution was selected for both absolute and relative fluctuations.

279 The animations of the two largest patches (Appendix S3, largest patch gif animations) qualitatively shows
280 the nature of fluctuations and if the state of the forest is connected or not. If the largest patch is always
281 the same patch over time, the forest is probably not fragmented; this happens for regions with RS_{max} of
282 more than 40% such as AF2 (Madagascar), NA1 (North America), and OC3 (Malaysia). In the regions with
283 RS_{max} between 40% and 30% the identity of the largest patch could change or stay the same in time. For
284 OC7 (Java) the largest patch changes and for AF1 (Africa mainland) it stays the same. Only for EUAS1
285 (Eurasia mainland) we observed that the two largest patches are always the same, implying that this region
286 is probably composed of two independent domains and should be divided in further studies. The regions
287 with RS_{max} less than 25%: SAST2 (Cuba) and EUAS3 (United Kingdom), the largest patch always changes
288 reflecting their fragmented state. In the case of SEAS2 (Philippines) a transition is observed, with the
289 identity of the largest patch first variable, and then constant after 2010.

290 The results of quantile regressions are identical for ΔRS_{max} and ΔS_{max} (Appendix S4, table S4). Among the
291 biggest regions, Africa (AF1) has upper and lower quantiles with significantly negative slopes, but the lower
292 quantile slope is lower, implying that negative fluctuations and variance are increasing (Figure 4). Eurasia
293 mainland (EUAS1) has only the upper quantile significant with a positive slope, suggesting an increase in the
294 variance. North America mainland (NA1) exhibits a significant lower quantile with positive slope, implying
295 decreasing variance. Finally, for mainland Australia, all quantiles are significant, and the slope of the lower
296 quantiles is greater than the upper ones, showing that variance is decreasing (Appendix S4, figure S10).
297 These results are summarized in Table 1.

298 The conditions that indicate that a region is near a critical fragmentation threshold are that patch size
299 distributions follow a power law; temporal ΔRS_{max} fluctuations follow a power law; variance of ΔRS_{max} is
300 increasing in time; and skewness is negative. All these conditions were true only for Africa mainland (AF1)
301 and South America tropical & subtropical (SAST1).

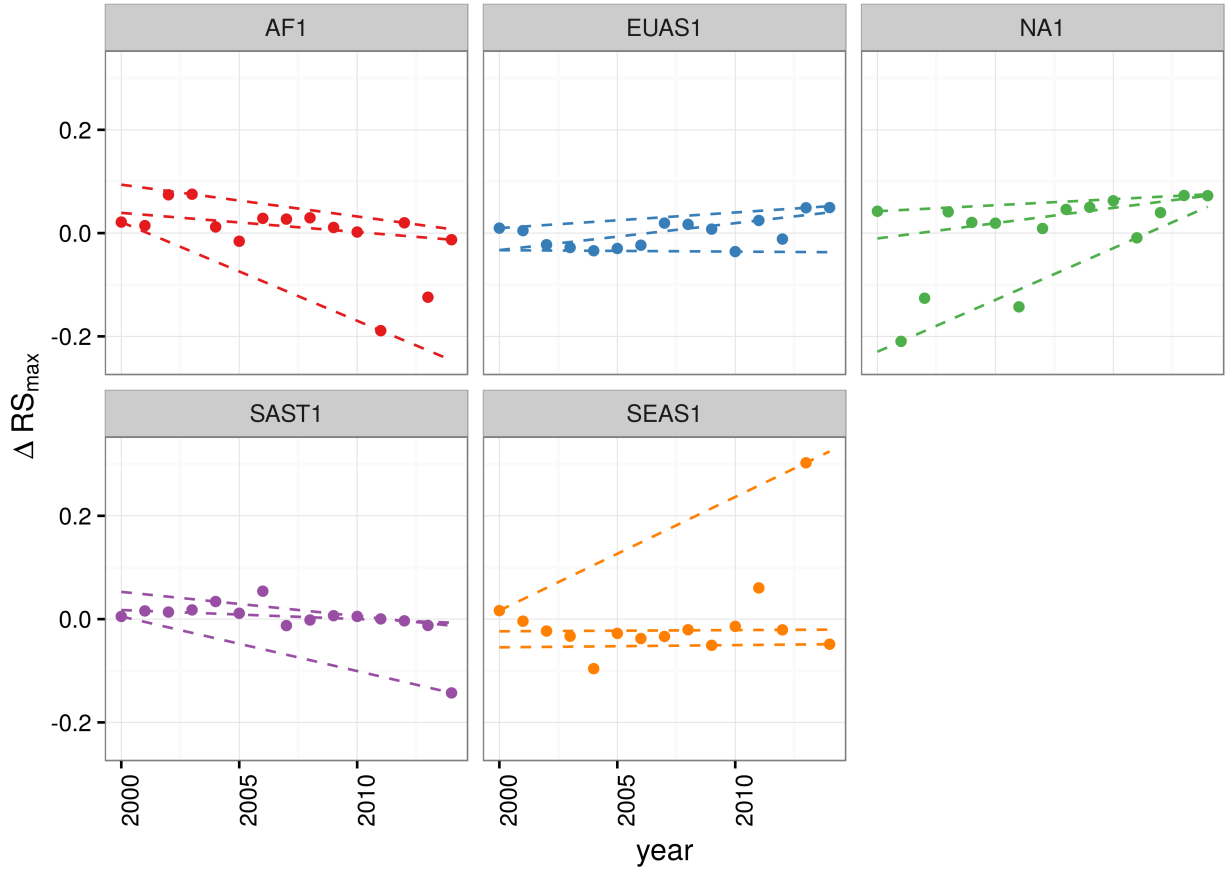


Figure 4: Largest patch fluctuations for regions with total forest area $> 10^7 \text{ km}^2$ across years. The patch sizes are relative to the total forest area of the same year. Dashed lines are 90%, 50% and 10% quantile regressions, to show if fluctuations were increasing. The regions are AF1: Africa mainland, EUAS1: Eurasia mainland, NA1: North America mainland, SAST1: South America tropical and subtropical, SEAS1: Southeast Asia mainland.

Table 1: Regions and indicators of closeness to a critical fragmentation threshold. Where, RS_{max} is the largest patch divided by the total forest area, ΔRS_{max} are the fluctuations of RS_{max} around the mean, skewness was calculated for RS_{max} and the increase or decrease in the variance was estimated using quantile regressions, NS means the results were non-significant. The conditions that determine the closeness to a threshold are

Region	Description	Average	Patch Size			
		RS_{max}	Distrib	ΔRS_{max}	Distrib.	Skewness
AF1	Africa mainland	0.36	Power	Power	-1.8630	Increase
AF2	Madagascar	0.65	Power	Power	-0.2478	NS
EUAS1	Eurasia, mainland	0.36	LogNormal	Exp	0.4016	Increase
EUAS2	Japan	0.94	Power	Power	0.0255	NS
EUAS3	United Kingdom	0.07	Power	Power	2.1330	NS
NA1	North America, mainland	0.71	Power	Power	-1.5690	Decrease
NA5	Newfoundland	0.87	Power	Power	-0.7411	NS
OC1	Australia, Mainland	0.28	Power	Power	0.0685	Decrease
OC2	New Guinea	0.97	Power	Exp	0.1321	Decrease
OC3	Malaysia/Kalimantan	0.97	Power	Exp	-0.9633	NS
OC4	Sumatra	0.92	Power	Power	1.3150	Increase
OC5	Sulawesi	0.87	Power	Power	-0.3863	NS
OC6	New Zealand South Island	0.76	Power	Exp	-0.6683	NS
OC7	Java	0.38	Power	Exp	-0.1948	NS
OC8	New Zealand North Island	0.75	Power	Exp	0.2940	NS
SAST1	South America, Tropical and subtropical forest up to Mexico	0.68	Power	Power	-2.7760	Increase
SAST2	Cuba	0.21	Power	Power	0.2751	NS
SAT1	South America, Temperate forest	0.60	Power	Power	-1.5070	Decrease
SEAS1	Southeast Asia, Mainland	0.40	Power	Power	3.0030	NS
SEAS2	Philippines	0.54	Power	Power	0.3113	Increase

302 Discussion

303 We found that the forest patch distribution of most regions of the world followed power laws spanning
 304 seven orders of magnitude. These include tropical rainforest, boreal and temperate forest. Power laws have
 305 previously been found for several kinds of vegetation, but never at global scales as in this study. Interestingly,
 306 Eurasia does not follow a power law, but it is a geographically extended region, consisting of different domains
 307 (as we observed in the largest patch animations, Appendix S2). It is known that the union of two independent
 308 power law distributions produces a lognormal distribution (Rooij *et al.* 2013). Future studies should split
 309 this region into two or more new regions, and test if the underlying distributions are power laws.

310 Several mechanisms have been proposed for the emergence of power laws in forest: the first is related self
 311 organized criticality (SOC), when the system is driven by its internal dynamics to a critical state; this has
 312 been suggested mainly for fire-driven forests (Zinck & Grimm 2009; Hantson, Pueyo & Chuvieco 2015).

313 Real ecosystems do not seem to meet the requirements of SOC dynamics: their dynamics are influenced by
314 external forces, and interactions are non-homogeneous (i.e. vary from place to place) (Sole, Alonso & Mckane
315 2002). Moreover, SOC requires a memory effect: fire scars in a site should accumulate and interfere with
316 the propagation of a new fire. Pueyo et al. (2010) did not find such effect for tropical forests, and suggest
317 that other mechanisms might produce the observed power laws. Other studies have also found that SOC
318 models do not reproduce the patterns of observed fires (McKenzie & Kennedy 2012). Thus a mechanism
319 which resembles SOC, i.e. with a double separation of scales, does not seem a plausible explanation for the
320 global forest dynamics.

321 The mechanism suggested by Pueyo et al. (2010) is isotropic percolation, when a system is near the critical
322 point power law structures arise. This is equivalent to the random forest model that we explained previously,
323 and requires the tuning of an external environmental condition to carry the system to this point. We did not
324 expect forest growth to be a random process at local scales, but it is possible that combinations of factors
325 cancel out to produce seemingly random forest dynamics at large scales. If this is the case the power law
326 exponent should be theoretically near $\alpha = 2.055$, this is close but outside the confidence interval we observed
327 (1.898 - 1.920), and thus other explanations are needed.

328 The third mechanism suggested as the cause of pervasive power laws in patch size distribution is facilitation
329 (Manor & Shnerb 2008; Irvine, Bull & Keeling 2016): a patch surrounded by forest will have a smaller
330 probability of been deforested or degraded than an isolated patch. We hypothesize that models that include
331 facilitation could explain the patterns observed here. The model of Scanlon et al. (2007) represented the
332 dynamics of savanna trees includes a global constraint (mean rainfall), a local facilitation mechanism, and
333 two states (tree/non-tree), producing power laws across a rainfall gradient without the need for tuning an
334 external parameter. The results for this model showed an $\alpha = 1.34$ which is also different from our results.
335 Another model but with three states (tree/non-tree/degraded), including local facilitation and grazing, was
336 also used to obtain power laws patch distributions without external tuning, and exhibited deviations from
337 power laws at high grazing pressures (Kéfi et al. 2007). The values of the power law exponent α obtained
338 for this model are dependent on the intensity of facilitation, when facilitation is more intense the exponent
339 is higher, but the maximal values they obtained are still lower than the ones we observed. The interesting
340 point is that the value of the exponent is dependent on the parameters, and thus the observed α might
341 be obtained with some parameter combination. Kéfi et al. (2007) proposed that a deviation in power law
342 behavior with the form of an exponential decay or cut-off could be a signal of a critical transition. At the
343 continental scales studied here, we did not observe exponential cut-offs, but did observe other signals of a
344 transition. This confirms previous results (Weerman et al. 2012; Kéfi et al. 2014) showing that different

345 mechanisms can produce seemingly different spatial patterns near the transition, and that early warnings
346 based only on spatial patterns are not universal for all systems.

347 It has been suggested that a combination of spatial and temporal indicators could more reliably detect
348 critical transitions (Kéfi *et al.* 2014). In this study, we combined five criteria to detect the closeness to a
349 fragmentation threshold. Two of them were spatial: the forest patch size distribution, and the proportion
350 of the largest patch relative to total forest area (RS_{max}). The other three were the distribution of temporal
351 fluctuations in the largest patch size, the trend in the variance, and the skewness of the fluctuations. Each
352 one of these is not a strong individual predictor, but their combination gives us an increased degree of
353 confidence about the system being close to a critical transition.

354 We found that only the tropical forest of Africa and South America met all five criteria, and thus seem to be
355 near a critical fragmentation threshold. This confirms previous studies that point to this two tropical areas
356 as the most affected by deforestation (Hansen *et al.* 2013), but our method fails to detect that Southeast Asia
357 was also in the first places of deforestation. One of the reasons would be that the MODIS dataset does not
358 detect if native forest is replaced by agroindustrial tree plantations like oil palms, that is the principal driver
359 of deforestation in this area (Malhi *et al.* 2014). Thus a refined dataset to determine forest patches which
360 integrates different kinds of information about land use, protected areas, forest type, is needed (Hansen *et*
361 *al.* 2014).

362 Of these two areas, Africa seems to be more affected, because the proportion of the largest patch relative to
363 total forest area (RS_{max}) is near 30%, which could indicate that the transition is already started. Moreover,
364 this region was estimated to be potentially bistable, with the possibility to completely transform into a
365 savanna (Staver, Archibald & Levin 2011). The region of South America tropical forest has a RS_{max} of
366 more than 60% suggesting that the fragmentation transition is approaching but not yet started. The island
367 of Philippines (SEAS2) seems to be an example of a critical transition from an unconnected to a connected
368 state, the early warning signals can be qualitatively observed: a big fluctuation in a negative direction
369 precedes the transition and then RS_{max} stabilizes over 60%. This confirms that the early warning indicators
370 proposed here work in the correct direction.

371 At low levels of habitat reduction, species population will decline proportionally; this can happen even when
372 the habitat fragments retain connectivity. As habitat reduction continues, the critical threshold is approached
373 and connectivity will have large fluctuations (Brook *et al.* 2013). This could trigger several synergistic
374 effects: populations fluctuations and the possibility of extinctions will rise, increasing patch isolation and
375 decreasing connectivity (Brook *et al.* 2013). This positive feedback mechanism will be enhanced when the
376 fragmentation threshold is reached, resulting in the loss of most habitat specialist species at a landscape

377 scale (Pardini *et al.* 2010). Some authors argue that since species have heterogeneous responses to habitat
378 loss and fragmentation, and biotic dispersal is limited, the importance of thresholds is restricted to local
379 scales or even that its existence is questionable (Brook *et al.* 2013). Fragmentation is by definition a
380 local process that at some point produces emergent phenomena over the entire landscape, even if the area
381 considered is infinite (Oborny, Meszéna & Szabó 2005). In addition, after a region's fragmentation threshold
382 connectivity decreases, there is still a large and internally well connected patch that can maintain sensitive
383 species (Martensen *et al.* 2012). What is the time needed for these large patches to become fragmented, and
384 pose a real danger of extinction to a myriad of sensitive species? If a forest is already in a fragmented state, a
385 second critical transition from forest to non-forest could happen, this was called the desertification transition
386 (Corrado *et al.* 2014). Considering the actual trends of habitat loss, and studying the dynamics of non-forest
387 patches—instead of the forest patches as we did here—the risk of this kind of transition could be estimated.
388 To improve the estimation of non-forest patches other data set as the MODIS cropland probability should be
389 incorporated (Sexton *et al.* 2015). The simple models proposed previously could also be used to estimate if
390 these thresholds are likely to be continuous and reversible or discontinuous and often irreversible (Weissmann
391 & Shnerb 2016), and the degree of protection (e.g. using the set-asides strategy Banks-Leite *et al.* (2014))
392 than would be necessary to stop this trend.

393 The effectiveness of landscape management is related to the degree of fragmentation, and the criteria to
394 direct reforestation efforts could be focused on regions near a transition (Oborny *et al.* 2007). Regions that
395 are in an unconnected state require large efforts to recover a connected state, but regions that are near a
396 transition could be easily pushed to a connected state; feedbacks due to facilitation mechanisms might help
397 to maintain this state. If the largest patch is always the same patch over time, the forest is probably not
398 fragmented. This patch could represent a core area for conservation, because it maintains the connectivity
399 of the whole region. The dynamical fragmentation analysis that we did could be performed at smaller scales
400 that would be more amenable to be managed for conservation, and their results could be readily applicable
401 to modify the fragmentation of an area.

402 Crossing the fragmentation critical point in forests could have negative effects on biodiversity and ecosystem
403 services (Haddad *et al.* 2015), but it could also produce feedback loops at different levels of the biological
404 hierarchy. This means that a critical transition produced at a continental scale could have effects at the level
405 of communities, food webs, populations, phenotypes and genotypes (Barnosky *et al.* 2012). All these effects
406 interact with climate change, thus there is a potential production of cascading effects that could lead to a
407 global collapse. Therefore, even if critical thresholds are reached only in some forest regions at a continental
408 scale, a cascading effect with global consequences could still be produced, and may contribute to reach a

409 planetary tipping point (Reyer *et al.* 2015). The risk of such event will be higher if the dynamics of separate
410 continental regions are coupled (Lenton & Williams 2013). Using the time series obtained in this work the
411 coupling of the continental could be further investigated. It has been proposed that to assess the probability
412 of a global scale shift, different small scale ecosystems should be studied in parallel (Barnosky *et al.* 2012).
413 As forest comprises a major proportion of such ecosystems, we think that the transition of forests could be
414 used as a proxy for all the underling changes and as a successful predictor of a planetary tipping point.

415 Supporting information

416 **Appendix S1:** Supplementary data, Csv text file with model fits for patch size distribution, and model
417 selection for all the regions.

418 **Appendix S2:** Gif Animations of a forest model percolation. These are animations showing the subcritical,
419 critical, and super critical states.

420 **Appendix S3:** Gif Animations of largest patches. These show the temporal dynamics of the two largest
421 patches.

422 **Appendix S4:** Tables and figures.

423 *Table S1:* Proportion of Power law models not rejected by the goodness of fit test at $p \leq 0.05$ level.

424 *Table S2:* Generalized least squares fit by maximizing the restricted log-likelihood.

425 *Table S3:* Simultaneous Tests for General Linear Hypotheses of the power law exponent.

426 *Table S4:* Quantile regressions of the proportion of largest patch area vs year.

427 *Table S5:* Unbiased estimation of skewness for absolute largest patch fluctuations and relative fluctuations.

428 *Table S6:* Model selection using Akaike criterion for largest patch fluctuations in absolute values

429 *Table S7:* Model selection for fluctuation of largest patch in relative to total forest area.

430 *Figure S1:* Regions for Africa (AF), 1 Mainland, 2 Madagascar.

431 *Figure S2:* Regions for Eurasia (EUAS), 1 Mainland, 2 Japan, 3 United Kingdom.

432 *Figure S3:* Regions for North America (NA), 1 Mainland, 5 Newfoundland.

433 *Figure S4:* Regions for Australia and islands (OC), 1 Australia mainland; 2 New Guinea; 3 Malaysia/Kalimantan;
434 4 Sumatra; 5 Sulawesi; 6 New Zealand south island; 7 Java; 8 New Zealand north island.

- 435 *Figure S5*: Regions for South America, SAST1 Tropical and subtropical forest up to Mexico; SAST2 Cuba;
436 SAT1 South America, Temperate forest.
- 437 *Figure S6*: Regions for Southeast Asia (SEAS), 1 Mainland; 2 Philippines.
- 438 *Figure S7*: Proportion of best models selected for patch size distributions using the Akaike criterion.
- 439 *Figure S8*: Power law exponents for forest patch distributions by year.
- 440 *Figure S9*: Largest patch proportion relative to total forest area RS_{max} , for regions with total forest area
441 less than 10^7 km^2 .
- 442 *Figure S10*: Fluctuations of largest patch for regions with total forest area less than 10^7 km^2 . The patch
443 sizes are relativized to the total forest area for that year.

444 Data Accessibility

- 445 The patch size files for all years and regions used here, and all the R and Matlab scripts are available at
446 figshare <http://dx.doi.org/10.6084/m9.figshare.4263905>.

447 Acknowledgments

- 448 LAS and SRD are grateful to the National University of General Sarmiento for financial support. This work
449 was partially supported by a grant from CONICET (PIO 144-20140100035-CO).

450 References

- 451 Allington, G.R.H. & Valone, T.J. (2010) Reversal of desertification: The role of physical and chemical soil
452 properties. *Journal of Arid Environments*, **74**, 973–977.
- 453 Banks-Leite, C., Pardini, R., Tambosi, L.R., Pearse, W.D., Bueno, A.A., Bruscagin, R.T., Condez, T.H.,
454 Dixo, M., Igari, A.T., Martensen, A.C. & Metzger, J.P. (2014) Using ecological thresholds to evaluate the
455 costs and benefits of set-asides in a biodiversity hotspot. *Science*, **345**, 1041–1045.
- 456 Barnosky, A.D., Hadly, E.A., Bascompte, J., Berlow, E.L., Brown, J.H., Fortelius, M., Getz, W.M., Harte, J.,
457 Hastings, A., Marquet, P.A., Martinez, N.D., Mooers, A., Roopnarine, P., Vermeij, G., Williams, J.W., Gille-
458 spie, R., Kitzes, J., Marshall, C., Matzke, N., Mindell, D.P., Revilla, E. & Smith, A.B. (2012) Approaching

- 459 a state shift in Earth's biosphere. *Nature*, **486**, 52–58.
- 460 Bascompte, J. & Solé, R.V. (1996) Habitat fragmentation and extinction thresholds in spatially explicit
461 models. *Journal of Animal Ecology*, **65**, 465–473.
- 462 Bazant, M.Z. (2000) Largest cluster in subcritical percolation. *Physical Review E*, **62**, 1660–1669.
- 463 Belward, A.S. (1996) *The IGBP-DIS Global 1 Km Land Cover Data Set “DISCover”: Proposal and Imple-*
464 *mentation Plans : Report of the Land Recover Working Group of IGBP-DIS*. IGBP-DIS Office.
- 465 Benedetti-Cecchi, L., Tamburello, L., Maggi, E. & Bulleri, F. (2015) Experimental Perturbations Modify the
466 Performance of Early Warning Indicators of Regime Shift. *Current biology*, **25**, 1867–1872.
- 467 Bestelmeyer, B.T., Ellison, A.M., Fraser, W.R., Gorman, K.B., Holbrook, S.J., Laney, C.M., Ohman, M.D.,
468 Peters, D.P.C., Pillsbury, F.C., Rassweiler, A., Schmitt, R.J. & Sharma, S. (2011) Analysis of abrupt tran-
469 sitions in ecological systems. *Ecosphere*, **2**, 129.
- 470 Boettiger, C. & Hastings, A. (2012) Quantifying limits to detection of early warning for critical transitions.
471 *Journal of The Royal Society Interface*, **9**, 2527–2539.
- 472 Bonan, G.B. (2008) Forests and Climate Change: Forcings, Feedbacks, and the Climate Benefits of Forests.
473 *Science*, **320**, 1444–1449.
- 474 Botet, R. & Ploszajczak, M. (2004) Correlations in Finite Systems and Their Universal Scaling Properties.
475 *Nonequilibrium physics at short time scales: Formation of correlations* (ed K. Morawetz), pp. 445–466.
476 Springer-Verlag, Berlin Heidelberg.
- 477 Brook, B.W., Ellis, E.C., Perring, M.P., Mackay, A.W. & Blomqvist, L. (2013) Does the terrestrial biosphere
478 have planetary tipping points? *Trends in Ecology & Evolution*.
- 479 Burnham, K. & Anderson, D.R. (2002) *Model selection and multi-model inference: A practical information-*
480 *theoretic approach*, 2nd. ed. Springer-Verlag, New York.
- 481 Canfield, D.E., Glazer, A.N. & Falkowski, P.G. (2010) The Evolution and Future of Earth's Nitrogen Cycle.
482 *Science*, **330**, 192–196.
- 483 Carpenter, S.R., Cole, J.J., Pace, M.L., Batt, R., Brock, W.A., Cline, T., Coloso, J., Hodgson, J.R., Kitchell,
484 J.F., Seekell, D.A., Smith, L. & Weidel, B. (2011) Early Warnings of Regime Shifts: A Whole-Ecosystem
485 Experiment. *Science*, **332**, 1079–1082.
- 486 Clauset, A., Shalizi, C. & Newman, M. (2009) Power-Law Distributions in Empirical Data. *SIAM Review*,

- 487 51, 661–703.
- 488 Corrado, R., Cherubini, A.M. & Pennetta, C. (2014) Early warning signals of desertification transitions in
489 semiarid ecosystems. *Physical Review E - Statistical, Nonlinear, and Soft Matter Physics*, **90**, 62705.
- 490 Crowther, T.W., Glick, H.B., Covey, K.R., Bettigole, C., Maynard, D.S., Thomas, S.M., Smith, J.R., Hintler,
491 G., Duguid, M.C., Amatulli, G., Tuanmu, M.-N., Jetz, W., Salas, C., Stam, C., Piotto, D., Tavani, R., Green,
492 S., Bruce, G., Williams, S.J., Wiser, S.K., Huber, M.O., Hengeveld, G.M., Nabuurs, G.-J., Tikhonova, E.,
493 Borchardt, P., Li, C.-F., Powrie, L.W., Fischer, M., Hemp, A., Homeier, J., Cho, P., Vibrans, A.C., Umunay,
494 P.M., Piao, S.L., Rowe, C.W., Ashton, M.S., Crane, P.R. & Bradford, M.A. (2015) Mapping tree density at
495 a global scale. *Nature*, **525**, 201–205.
- 496 Dai, L., Vorselen, D., Korolev, K.S. & Gore, J. (2012) Generic Indicators for Loss of Resilience Before a
497 Tipping Point Leading to Population Collapse. *Science*, **336**, 1175–1177.
- 498 DiMiceli, C., Carroll, M., Sohlberg, R., Huang, C., Hansen, M. & Townshend, J. (2015) Annual Global
499 Automated MODIS Vegetation Continuous Fields (MOD44B) at 250 m Spatial Resolution for Data Years
500 Beginning Day 65, 2000 - 2014, Collection 051 Percent Tree Cover, University of Maryland, College Park,
501 MD, USA.
- 502 Drake, J.M. & Griffen, B.D. (2010) Early warning signals of extinction in deteriorating environments. *Nature*,
503 **467**, 456–459.
- 504 Efron, B. & Tibshirani, R.J. (1994) *An Introduction to the Bootstrap*. Taylor & Francis, New York.
- 505 Filotas, E., Parrott, L., Burton, P.J., Chazdon, R.L., Coates, K.D., Coll, L., Haeussler, S., Martin, K.,
506 Nocentini, S., Puettmann, K.J., Putz, F.E., Simard, S.W. & Messier, C. (2014) Viewing forests through the
507 lens of complex systems science. *Ecosphere*, **5**, 1–23.
- 508 Foley, J.A., Ramankutty, N., Brauman, K.A., Cassidy, E.S., Gerber, J.S., Johnston, M., Mueller, N.D.,
509 O'Connell, C., Ray, D.K., West, P.C., Balzer, C., Bennett, E.M., Carpenter, S.R., Hill, J., Monfreda, C.,
510 Polasky, S., Rockström, J., Sheehan, J., Siebert, S., Tilman, D. & Zaks, D.P.M. (2011) Solutions for a
511 cultivated planet. *Nature*, **478**, 337–342.
- 512 Folke, C., Jansson, Å., Rockström, J., Olsson, P., Carpenter, S.R., Iii, F.S.C., Crépin, A.-S., Daily, G.,
513 Danell, K., Ebbesson, J., Elmquist, T., Galaz, V., Moberg, F., Nilsson, M., Österblom, H., Ostrom, E.,
514 Persson, Å., Peterson, G., Polasky, S., Steffen, W., Walker, B. & Westley, F. (2011) Reconnecting to the
515 Biosphere. *AMBIO*, **40**, 719–738.
- 516 Fung, T., O'Dwyer, J.P., Rahman, K.A., Fletcher, C.D. & Chisholm, R.A. (2016) Reproducing static and

- 517 dynamic biodiversity patterns in tropical forests: the critical role of environmental variance. *Ecology*, **97**,
518 1207–1217.
- 519 Gardner, R.H. & Urban, D.L. (2007) Neutral models for testing landscape hypotheses. *Landscape Ecology*,
520 **22**, 15–29.
- 521 Gastner, M.T., Oborny, B., Zimmermann, D.K. & Pruessner, G. (2009) Transition from Connected to Frag-
522 mented Vegetation across an Environmental Gradient: Scaling Laws in Ecotone Geometry. *The American
523 Naturalist*, **174**, E23–E39.
- 524 Gillespie, C.S. (2015) Fitting Heavy Tailed Distributions: The poweRlaw Package. *Journal of Statistical
525 Software*, **64**, 1–16.
- 526 Gilman, S.E., Urban, M.C., Tewksbury, J., Gilchrist, G.W. & Holt, R.D. (2010) A framework for community
527 interactions under climate change. *Trends in Ecology & Evolution*, **25**, 325–331.
- 528 Goldstein, M.L., Morris, S.A. & Yen, G.G. (2004) Problems with fitting to the power-law distribution. *The
529 European Physical Journal B - Condensed Matter and Complex Systems*, **41**, 255–258.
- 530 Haddad, N.M., Brudvig, L.a., Clobert, J., Davies, K.F., Gonzalez, A., Holt, R.D., Lovejoy, T.E., Sexton,
531 J.O., Austin, M.P., Collins, C.D., Cook, W.M., Damschen, E.I., Ewers, R.M., Foster, B.L., Jenkins, C.N.,
532 King, a.J., Laurance, W.F., Levey, D.J., Margules, C.R., Melbourne, B.a., Nicholls, a.O., Orrock, J.L.,
533 Song, D.-X. & Townshend, J.R. (2015) Habitat fragmentation and its lasting impact on Earth's ecosystems.
534 *Science Advances*, **1**, 1–9.
- 535 Hansen, M., Potapov, P., Margono, B., Stehman, S., Turubanova, S. & Tyukavina, A. (2014) Response to
536 Comment on “High-resolution global maps of 21st-century forest cover change”. *Science*, **344**, 981.
- 537 Hansen, M.C., Potapov, P.V., Moore, R., Hancher, M., Turubanova, S.A., Tyukavina, A., Thau, D., Stehman,
538 S.V., Goetz, S.J., Loveland, T.R., Kommareddy, A., Egorov, A., Chini, L., Justice, C.O. & Townshend, J.R.G.
539 (2013) High-Resolution Global Maps of 21st-Century Forest Cover Change. *Science*, **342**, 850–853.
- 540 Hantson, S., Pueyo, S. & Chuvieco, E. (2015) Global fire size distribution is driven by human impact and
541 climate. *Global Ecology and Biogeography*, **24**, 77–86.
- 542 Harris, T.E. (1974) Contact interactions on a lattice. *The Annals of Probability*, **2**, 969–988.
- 543 Hastings, A. & Wysham, D.B. (2010) Regime shifts in ecological systems can occur with no warning. *Ecology
544 Letters*, **13**, 464–472.
- 545 He, F. & Hubbell, S. (2003) Percolation Theory for the Distribution and Abundance of Species. *Physical*

- 546 *Review Letters*, **91**, 198103.
- 547 Hinrichsen, H. (2000) Non-equilibrium critical phenomena and phase transitions into absorbing states. *Advances in Physics*, **49**, 815–958.
- 549 Irvine, M.A., Bull, J.C. & Keeling, M.J. (2016) Aggregation dynamics explain vegetation patch-size distributions. *Theoretical Population Biology*, **108**, 70–74.
- 551 Keitt, T.H., Urban, D.L. & Milne, B.T. (1997) Detecting critical scales in fragmented landscapes. *Conservation Ecology*, **1**, 4.
- 553 Kéfi, S., Guttal, V., Brock, W.A., Carpenter, S.R., Ellison, A.M., Livina, V.N., Seekell, D.A., Scheffer, M.,
554 Nes, E.H. van & Dakos, V. (2014) Early Warning Signals of Ecological Transitions: Methods for Spatial
555 Patterns. *PLoS ONE*, **9**, e92097.
- 556 Kéfi, S., Rietkerk, M., Alados, C.L., Pueyo, Y., Papanastasis, V.P., ElAich, A. & Ruiter, P.C. de. (2007)
557 Spatial vegetation patterns and imminent desertification in Mediterranean arid ecosystems. *Nature*, **449**,
558 213–217.
- 559 Kitzberger, T., Aráoz, E., Gowda, J.H., Mermoz, M. & Morales, J.M. (2012) Decreases in Fire Spread Prob-
560 ability with Forest Age Promotes Alternative Community States, Reduced Resilience to Climate Variability
561 and Large Fire Regime Shifts. *Ecosystems*, **15**, 97–112.
- 562 Klaus, A., Yu, S. & Plenz, D. (2011) Statistical analyses support power law distributions found in neuronal
563 avalanches. (ed M Zochowski). *PloS one*, **6**, e19779.
- 564 Koenker, R. (2016) quantreg: Quantile Regression.
- 565 Leibold, M.A. & Norberg, J. (2004) Biodiversity in metacommunities: Plankton as complex adaptive sys-
566 tems? *Limnology and Oceanography*, **49**, 1278–1289.
- 567 Lenton, T.M. & Williams, H.T.P. (2013) On the origin of planetary-scale tipping points. *Trends in Ecology
& Evolution*, **28**, 380–382.
- 569 Loehle, C., Li, B.-L. & Sundell, R.C. (1996) Forest spread and phase transitions at forest-prairie ecotones in
570 Kansas, U.S.A. *Landscape Ecology*, **11**, 225–235.
- 571 Malhi, Y., Gardner, T.A., Goldsmith, G.R., Silman, M.R. & Zelazowski, P. (2014) Tropical Forests in the
572 Anthropocene. *Annual Review of Environment and Resources*, **39**, 125–159.
- 573 Manor, A. & Shnerb, N.M. (2008) Origin of pareto-like spatial distributions in ecosystems. *Physical Review*

- 574 *Letters*, **101**, 268104.
- 575 Martensen, A.C., Ribeiro, M.C., Banks-Leite, C., Prado, P.I. & Metzger, J.P. (2012) Associations of Forest
576 Cover, Fragment Area, and Connectivity with Neotropical Understory Bird Species Richness and Abundance.
577 *Conservation Biology*, **26**, 1100–1111.
- 578 Martín, P.V., Bonachela, J.A., Levin, S.A. & Muñoz, M.A. (2015) Eluding catastrophic shifts. *Proceedings
579 of the National Academy of Sciences*, **112**, E1828–E1836.
- 580 McKenzie, D. & Kennedy, M.C. (2012) Power laws reveal phase transitions in landscape controls of fire
581 regimes. *Nat Commun*, **3**, 726.
- 582 Mitchell, M.G.E., Suarez-Castro, A.F., Martinez-Harms, M., Maron, M., McAlpine, C., Gaston, K.J., Jo-
583 hansen, K. & Rhodes, J.R. (2015) Reframing landscape fragmentation's effects on ecosystem services. *Trends
584 in Ecology & Evolution*, **30**, 190–198.
- 585 Naito, A.T. & Cairns, D.M. (2015) Patterns of shrub expansion in Alaskan arctic river corridors suggest
586 phase transition. *Ecology and Evolution*, **5**, 87–101.
- 587 Oborny, B., Meszéna, G. & Szabó, G. (2005) Dynamics of Populations on the Verge of Extinction. *Oikos*,
588 **109**, 291–296.
- 589 Oborny, B., Szabó, G. & Meszéna, G. (2007) Survival of species in patchy landscapes: percolation in space
590 and time. *Scaling biodiversity*, pp. 409–440. Cambridge University Press.
- 591 Ochoa-Quintero, J.M., Gardner, T.A., Rosa, I., de Barros Ferraz, S.F. & Sutherland, W.J. (2015) Thresholds
592 of species loss in Amazonian deforestation frontier landscapes. *Conservation Biology*, **29**, 440–451.
- 593 Ódor, G. (2004) Universality classes in nonequilibrium lattice systems. *Reviews of Modern Physics*, **76**,
594 663–724.
- 595 Pardini, R., Bueno, A. de A., Gardner, T.A., Prado, P.I. & Metzger, J.P. (2010) Beyond the Fragmentation
596 Threshold Hypothesis: Regime Shifts in Biodiversity Across Fragmented Landscapes. *PLoS ONE*, **5**, e13666.
- 597 Pinheiro, J., Bates, D., DebRoy, S., Sarkar, D. & R Core Team. (2016) *nlme: Linear and Nonlinear Mixed
598 Effects Models*.
- 599 Pueyo, S., de Alencastro Graça, P.M.L., Barbosa, R.I., Cots, R., Cardona, E. & Fearnside, P.M. (2010)
600 Testing for criticality in ecosystem dynamics: the case of Amazonian rainforest and savanna fire. *Ecology*

- 601 *Letters*, **13**, 793–802.
- 602 R Core Team. (2015) R: A Language and Environment for Statistical Computing.
- 603 Reyer, C.P.O., Rammig, A., Brouwers, N. & Langerwisch, F. (2015) Forest resilience, tipping points and
604 global change processes. *Journal of Ecology*, **103**, 1–4.
- 605 Rockstrom, J., Steffen, W., Noone, K., Persson, A., Chapin, F.S., Lambin, E.F., Lenton, T.M., Scheffer, M.,
606 Folke, C., Schellnhuber, H.J., Nykvist, B., Wit, C.A. de, Hughes, T., Leeuw, S. van der, Rodhe, H., Sorlin,
607 S., Snyder, P.K., Costanza, R., Svedin, U., Falkenmark, M., Karlberg, L., Corell, R.W., Fabry, V.J., Hansen,
608 J., Walker, B., Liverman, D., Richardson, K., Crutzen, P. & Foley, J.A. (2009) A safe operating space for
609 humanity. *Nature*, **461**, 472–475.
- 610 Rooij, M.M.J.W. van, Nash, B., Rajaraman, S. & Holden, J.G. (2013) A Fractal Approach to Dynamic
611 Inference and Distribution Analysis. *Frontiers in Physiology*, **4**.
- 612 Saravia, L.A. & Momo, F.R. (2017) Biodiversity collapse and early warning indicators in a spatial phase
613 transition between neutral and niche communities. *PeerJ PrePrints*, **5**, e1589v4.
- 614 Scanlon, T.M., Caylor, K.K., Levin, S.A. & Rodriguez-iturbe, I. (2007) Positive feedbacks promote power-law
615 clustering of Kalahari vegetation. *Nature*, **449**, 209–212.
- 616 Scheffer, M., Bascompte, J., Brock, W.A., Brovkin, V., Carpenter, S.R., Dakos, V., Held, H., Nes, E.H.V.,
617 Rietkerk, M. & Sugihara, G. (2009) Early-warning signals for critical transitions. *Nature*, **461**, 53–59.
- 618 Scheffer, M., Walker, B., Carpenter, S., Foley, J. a, Folke, C. & Walker, B. (2001) Catastrophic shifts in
619 ecosystems. *Nature*, **413**, 591–596.
- 620 Seidler, T.G. & Plotkin, J.B. (2006) Seed Dispersal and Spatial Pattern in Tropical Trees. *PLoS Biology*, **4**,
621 e344.
- 622 Sexton, J.O., Noojipady, P., Song, X.-P., Feng, M., Song, D.-X., Kim, D.-H., Anand, A., Huang, C., Channan,
623 S., Pimm, S.L. & Townshend, J.R. (2015) Conservation policy and the measurement of forests. *Nature
624 Climate Change*, **6**, 192–196.
- 625 Sole, R.V., Alonso, D. & Mckane, A. (2002) Self-organized instability in complex ecosystems. *Philosophical
626 transactions of the Royal Society of London. Series B, Biological sciences*, **357**, 667–681.
- 627 Solé, R.V. (2011) *Phase Transitions*. Princeton University Press.
- 628 Solé, R.V. & Bascompte, J. (2006) *Self-organization in complex ecosystems*. Princeton University Press, New

- 629 Jersey, USA.
- 630 Solé, R.V., Alonso, D. & Saldaña, J. (2004) Habitat fragmentation and biodiversity collapse in neutral
631 communities. *Ecological Complexity*, **1**, 65–75.
- 632 Solé, R.V., Bartumeus, F. & Gamarra, J.G.P. (2005) Gap percolation in rainforests. *Oikos*, **110**, 177–185.
- 633 Stauffer, D. & Aharony, A. (1994) *Introduction To Percolation Theory*. Taylor & Francis, London.
- 634 Staver, A.C., Archibald, S. & Levin, S.A. (2011) The Global Extent and Determinants of Savanna and Forest
635 as Alternative Biome States. *Science*, **334**, 230–232.
- 636 Vasilakopoulos, P. & Marshall, C.T. (2015) Resilience and tipping points of an exploited fish population over
637 six decades. *Global Change Biology*, **21**, 1834–1847.
- 638 Weerman, E.J., Van Belzen, J., Rietkerk, M., Temmerman, S., Kéfi, S., Herman, P.M.J. & Koppell, J.V.
639 de. (2012) Changes in diatom patch-size distribution and degradation in a spatially self-organized intertidal
640 mudflat ecosystem. *Ecology*, **93**, 608–618.
- 641 Weissmann, H. & Shnerb, N.M. (2016) Predicting catastrophic shifts. *Journal of Theoretical Biology*, **397**,
642 128–134.
- 643 Zhang, J.Y., Wang, Y., Zhao, X., Xie, G. & Zhang, T. (2005) Grassland recovery by protection from grazing
644 in a semi-arid sandy region of northern China. *New Zealand Journal of Agricultural Research*, **48**, 277–284.
- 645 Zinck, R.D. & Grimm, V. (2009) Unifying wildfire models from ecology and statistical physics. *The American
646 naturalist*, **174**, E170–85.
- 647 Zuur, A.F., Ieno, E.N., Walker, N., Saveliev, A.A. & Smith, G.M. (2009) *Mixed effects models and extensions
648 in ecology with R*. Springer New York, New York, NY.